Modeling of a Variable-BVR Rotary Valve Free Piston Expander/Compressor

Sergei Gusev * **Andres Hernandez** ** **Davide Ziviani** *
Martijn van den Broek *

* *Ghent University, Department of Flow, Heat and Combustion Mechanics, Graaf Karel de Goedelaan 5, Kortrijk, Belgium (e-mail: Sergei.Gusev@UGent.be, Davide.Ziviani@UGent.be, Martijn.vandenBroek@UGent.be).*
** *Ghent University, Department of Electrical Energy, Systems and Automation, Technologiepark 914 B-9052 Zwijnaarde, Belgium (e-mail: Andres.Hernandez@UGent.be)*

Abstract: The concept of a free-piston expansion/compression unit with a variable Built-in Volume Ratio (BVR) is proposed. This device has no crankshaft mechanism which provides a possibility to optimize the expansion process free of mechanical limitations. An additional degree of freedom is used, namely the rotation to control the in- and the outlet ports timing. Further, the operation in the expander mode will be described.
In most of the existing linear expanders/compressors, bouncing chambers or devices are used to reverse the piston movement at extreme positions. This approach is characterized by relatively high energy losses due to irreversibility of such a process. As an alternative, a fully controlled movement of the piston is proposed. This paper is focused on the control algorithm based on rules, which have been obtained and based on the insight in the system. Including the rotation timing, resulting in an optimal expansion process with an outlet pressure matching with the required one.

1. INTRODUCTION

Steady state operating volumetric compressors and expanders are widely studied machines. The challenge is to use such devices under strongly varying in- and outlet pressure and temperature conditions, especially at relatively high pressure ratios, which is frequently the case in waste heat recovery for non-stationary applications. For instance, the heat recovery from truck flue gases by means of an Organic Rankine Cycle (ORC) requires an expansion device with adjustable Built-in Volume Ratio (BVR). Fixed BVR machines cannot follow variations in the evaporating pressure caused by changes in both the flow rate and the temperature of the exhaust gases, resulting in a non-optimal operation of the system.

To overcome the lack of commercially available expanders, a novel variable-BVR expander has been proposed by the authors as an alternative to existing solutions, mainly conversion of compressors to expanders (Imran et al., 2016). Based on the results obtained during the tests performed on an ORC laboratory setup, the proposed idea intends to be a solution for challenges in expander technology established during these experiments.

The long-term objective is to develop a commercial unit meeting the requirements for a micro-scale ORC-system: inexpensive, scalable, flexible and efficient. The short-term objective, which has to be reached in the frame of the current project, is to develop a setup meant to validate

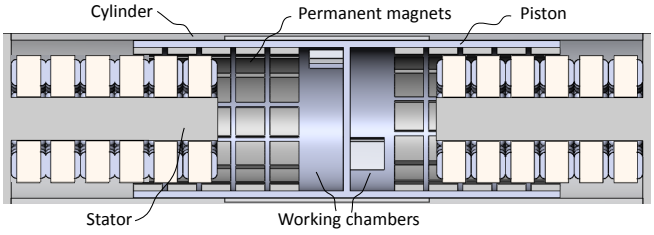

Fig. 1. Expander cutaway view

the behavior of the main components and to demonstrate the feasibility to synchronize the linear and the rotational movement of a piston in order to achieve any required volume ratio. A proposal for a patent has been filed.

In this paper, the first approach towards the design of a control strategy for the proposed machine, is reported. The mathematical modeling and the numerical results, which led to the consideration of a controller design, are presented and discussed.

2. NOVEL VARIABLE-BVR EXPANDER

The mechanical design and the operation principle of the test prototype with an embedded linear generator (Fig. 1) is described in previous publications (Gusev et al., 2016). The piston rotates while moving, closing and opening the

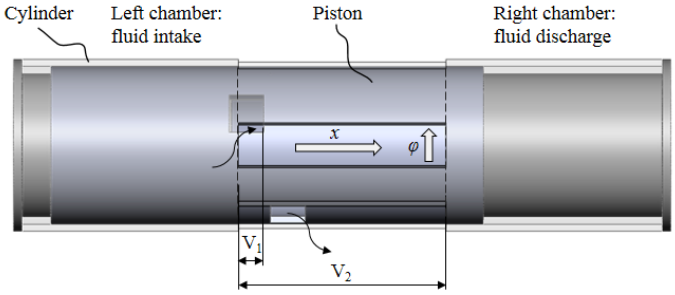

Fig. 2. Variable volume ratio

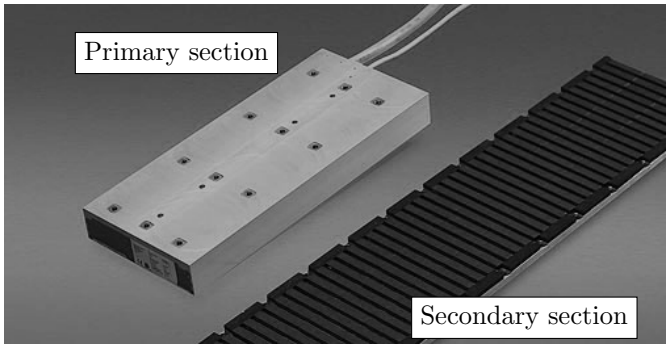

Fig. 3. Standard linear motor

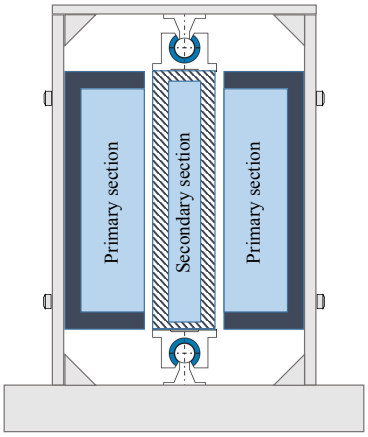

Fig. 4. Adjusted design

intake port at the required moment defined by the model. The built-in volumetric ratio can be expressed as:

$$BVR = \frac{V_2}{V_1} = \frac{1}{\chi}, \tag{1}$$

where V_1 is the volume at the moment of closing of the inlet port and V_2 is the volume of the working chamber after the expansion. The piston relative displacement χ corresponds with the volume V_1.

The $BVR = 10$ at $\chi = 0.1$ is shown in Fig. 2 when the leading-bottom corner of the piston skirt opening leaves the inlet opening of the cylinder. Since the rotation and translation of the piston have to be synchronized, the model is focused on the accurate definition and control of the piston position in both dimensions by means of rules, dictated by the thermodynamic model. The control coefficients, obtained from this model trigger the control sequence accelerating or decelerating the piston. The feedback signal is provided by the translation and the rotation encoders.

Since at the beginning of the prototype design, leakages are unavoidable and the discharge of expensive or toxic working fluids into the atmosphere is unacceptable, air is chosen as a working fluid.

In order to avoid complications with an embedded design, it was decided to separate translation and rotation movement and to use standard components. Several industrial linear motors operating in a brake mode are compared, its characteristics provided by the manufacturers are used as input for the model.

The chosen configuration is based on a standard linear motor consisting of a moving primary coil section and a secondary magnetic section (Fig. 2). In the adjusted design, two moving magnetic secondary sections are placed back-to-back on a linear guide system and two primary coil sections are fastened outside (Fig. 4). Such a configuration allows to equalize electromagnetic attraction forces and to reduce drastically the friction losses in the linear guiding system. Moreover, the maximal static force is twice the size, compared to a single-coil design for almost the same setup size and it is 6.2 kN in total. The inlet pressure applied to the piston can vary from 0.6 to 1.6 MPa. Other major setup parameters are summarized in Table 1.

Table 1. Main parameters of the designed test setup

Bore (m)	Stroke (m)	Frequency (Hz)	Moving mass (kg)
0.08	0.23 - 0.31	5 - 10	30

3. THE EQUATION OF MOTION

3.1 Translation

The model of the free-piston expander is based on the same approach as (Mikalsen and Roskilly, 2008). The dynamics of the piston translation is dictated by Newton's second law:

$$F_{p,cyl} - F_{p,dis} - F_{fr} - F_{el} = m_p \frac{d^2x}{dt^2}, \tag{2}$$

where $F_{p,cyl}$ and $F_{p,dis}$ are gas forces in opposing working chambers, the friction force F_{fr}, the electromagnetic force F_{el} and the piston mass m_p.

The gas forces are applied to the same central element and defined by the pressure profile of an expansion process (Fig. 5) which is simulated using the expander hybrid gray box model designed in previous studies. The CoolProp library connected to Python is used (Bell et al., 2014) in order to calculate thermodynamical parameters.

The working fluid entering the expander is cooled down since the expander wall temperature is typically between the in- and the outlet temperature of the working medium. At the end of the expansion, the heat flux reverses. This heat transfer from or to the expander walls is taken

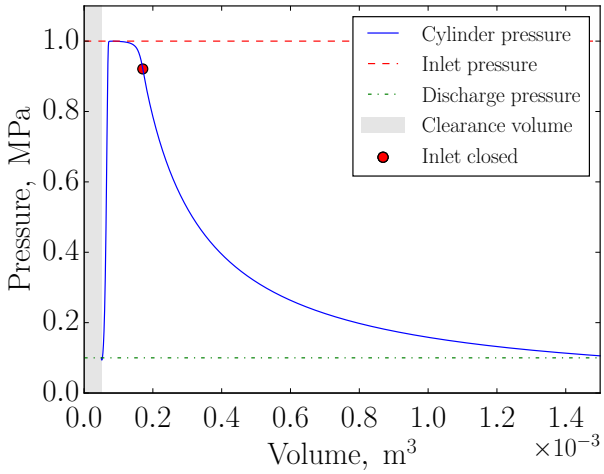

Fig. 5. pV-diagram

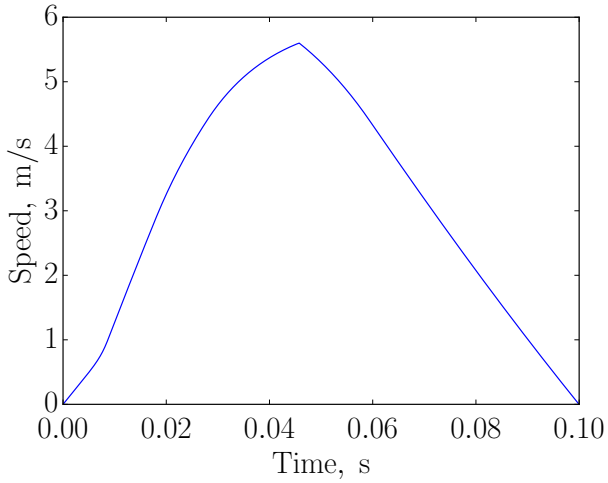

Fig. 6. Linear velocity profile

into account. The friction force F_{fr} is dependent on the speed of the piston. The correlation for dynamic friction behaviors of pneumatic cylinders obtained in (Tran and Yanada, 2013) is used. The heat produced by the friction is also incorporated into the model.

The translation speed changes under the applied electromagnetic force F_{el}, which is constant and acting alternately accelerating and decelerating the piston, in order to stop the piston at its extreme left and right positions, so all kinetic energy is absorbed and transformed into electricity. The approach is similar to (Petrichenko et al., 2015). The resulting equation can be written as follows:

$$F_{el}(t) = \frac{\pi D^2}{4}\left(p_{cyl}(t) - p_{dis}\right) - F_{fr}\left(\frac{dx}{dt}\right) - m_p\frac{d^2x}{dt^2}\,, \quad (3)$$

where D - is the piston diameter, p_{cyl} and p_{dis} are pressures in the working chamber and the discharge port respectively. The Equation 3 is used to control the drive of the linear motor, the position sensor is used for feedback of the piston position. The rotation is synchronized with the translation in order to obtain the required discharge pressure at the end of the expansion (Fig. 6).

3.2 Rotation

A servo motor attached to the expander on the opposite side of the linear generator side rotates the piston with an average frequency of 1/2 the frequency of the translation since there are two inlet and two outlet ports in each working chamber. The general equation for torque balance at the motor shaft can be written for the prototype as follows:

$$T_{el} = T_j + T_{fric}\,, \quad (4)$$

where T_{el} electromagnetic torque, T_j - inertia torque and T_{fric} - friction torque. The moment of inertia defining the inertia torque is the sum of moments of inertia of all components in the rotation train: the servo motor, the piston and shafts. These can be calculated using the sizes of the components used. These components rotate about the same axis and are have cylindric shape. The moment of inertia of a hollow cylinder is:

$$J = \frac{1}{8}m(D_{out}^2 + D_{in}^2)\,, \quad (5)$$

where m is the mass of the rotating component, D_{out} - the outer diameter, D_{in} - the inner one which is equal to zero for shafts and the servo motor rotor. The shaft mass and the diameter is relatively small and therefore can be neglected.

For the calculations of the friction torque, the same correlation as for the linear motion can be used (Tran and Yanada, 2013) with adjustments for the rotational motion by substitution of the peripheral speed of the piston instead of the linear one.

The resulting equation, used for the servo motor control can be written as follows:

$$T_{el}(t) = \frac{d^2\varphi}{dt^2}\left[\frac{1}{8}\left(m_{rot}D_{rot}^2 + m_{cyl}\left(D_{cyl,out}^2 + D_{cyl,in}^2\right)\right) + \right.$$
$$\left. + \frac{D_{cyl}}{2}F_{fric}\left(\frac{\varphi(t)}{dt}\right)\right], \quad (6)$$

where D_{rot} - is the servo motor rotor diameter, $D_{cyl,out}$ and $D_{cyl,in}$ are the outer and the inner diameter of the piston.

There is no influence op working pressures on the rotation since the in- and the outlet ports are placed axisymmetrically and therefore the pressure induced forces are compensated.

4. CONTROL STRATEGY

The control strategy here proposed corresponds to an algorithm designed based on the mechanical insight, where a set of rules are proposed to achieve the desired performance.

4.1 Intake and discharge.

The working medium enters the expander through a rectangular port formed by the openings in the housing and the skirts. The mass flow rate is dependent on the port area S, the pressure difference between the inlet pressure p_{su}

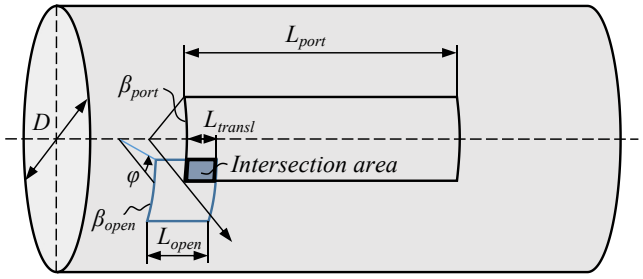

Fig. 7. Schematic of the port geometry.

Table 2. Inlet port and the skirt opening sizes

L_{open} (m)	L_{port} (m)	β_{open} (rad)	β_{port} (rad)
0.02	0.23	$\pi/12$	$\pi/12$

and the pressure in the cylinder p_{cyl}. The intersection area is changing according to the rotation and the translation of the piston (Fig. 7).

The position of the lower left corner of the cylinder wall opening is chosen as the reference point. The start of the intake process corresponds with the position of the piston when the lead-top corner of the skirt opening is at the reference point. A simplified algorithm defining the overlap of two rectangular openings is used to calculate the intersection area (Eq. 7):

$$\begin{aligned} S(t) = (&max(0, min(L_{transl}(t), L_{port}) \\ &- max(0, L_{transl}(t) - L_{open})) \times \\ &\times (max(0, min(\varphi(t), \beta_{port}) \\ &- max(0, \phi(t) - \beta_{open})) \cdot \frac{\pi D}{2} \cdot n \,, \end{aligned} \tag{7}$$

where n is the number of ports. There are two axisymmetric ports used in current configuration. The inlet port and the skirt opening sizes are shown in Table 2.

A similar model is applied to estimate the mass flow rate during the discharge process. The corresponding pressures p_{cyl} and p_{dis} are used.

4.2 Optimization criteria

Filling factor. The stroke length is defined in previous simulations and is kept constant. The piston movement profile under the applied forces defines the frequency of the machine, which must be maximized for a higher mass flow rate of the working medium. However, the higher the piston speed during the intake phase, the more difficult to maximize the inlet area for a higher filling factor. The definition of a filling factor is introduced by (Lemort et al., 2009) and means the measured flow rate divided by the displacement. Ideally, the density of the working fluid at the end of the intake is equal to the one at the inlet port. The actual density of the working fluid in the cylinder divided by the ideal one gives the indication of the intake efficiency.

$$\phi_{ff} = \frac{\rho_{cyl}}{\rho_{su}} \tag{8}$$

Table 3. Adjustable control parameters for different inlet pressures.

Pressure, MPa	$k1$	$k2$	$k3$	$k4$	$k5$	$k6$
1.0	0.41	1.05	0.426	0.242	0.15	0.006
0.6	0.75	1.09	1.0	0.242	0.15	0.007

A non-optimized velocity profile is shown on Fig. 6. As it can be seen on pV-diagram (Fig. 10), the inlet port closes relatively late causing a significant pressure drop of about 100 kPa at the end of the intake. The filling factor in this case is about 0.89.

After the optimization, the filling factor rises above the unity, which, beside the optimization, is caused by cooling down of the working fluid during the intake process due to a lower temperature of the expander. A normalized filling factor can be applied by using the actual temperature in the working chamber instead of the inlet temperature.

Intake efficiency. Another optimization criterion can be the intake efficiency expressed as a ratio of surface areas of the actual and ideal pV-diagrams from the opening of the inlet until it closes. After the rotation and translation adjustment, the values of 0.96 - 0.97 are obtained.

The linear motion and the rotation of the piston have to be synchronized in order to achieve the required BVR and a maximal inlet area during the intake. The maximal inlet area is theoretically achievable only if the motion of the piston is defined by square waves of both the rotation and the translation, which is impossible in practice due to a certain mass and the moment of inertia characterizing the piston. It is possible to approach such an ideal movement profile by reducing the piston acceleration while the inlet is open for more accurate timing control by rotation. The rotation has to be also adjusted.

Fig. 8 and Fig. 9 show the control algorithm for the piston linear movement and the rotation respectively. The adjustable parameters $k1$ - $k6$ allowing the pressure ratio of 1.0 and 0.6 MPa are shown in Table 3.

4.3 Translation control

Intake: $F_{em} = F_{nom} \cdot k1$ - the electromagnetic force is limited by the factor $k1$ during the inlet phase.

$p_{cyl} < p_{dis} \cdot k2$ - the piston is forced to move until the inlet port opens and the cylinder pressure starts to increase until a certain value defined by $k2$.

$F_{em} = -F_{del_p} + F_{fric}$ - the piston speed is kept constant as long as the inlet is open ($\varphi > \beta_{port} + \beta_{open}$). All forces are compensated by the electromagnetic one.

Acceleration: While the piston speed is lower then v_{max}, the nominal force (F_{nom}) is applied.

Brake: The electromagnetic force is adjusted so the piston reaches its extreme right position with $v = 0$ (Fig. 11). A PI-action can be applied at the end of the stroke in order to compensate a linear positioning error. It is important to avoid an overshoot since it means a mechanical impact of the piston on the stator.

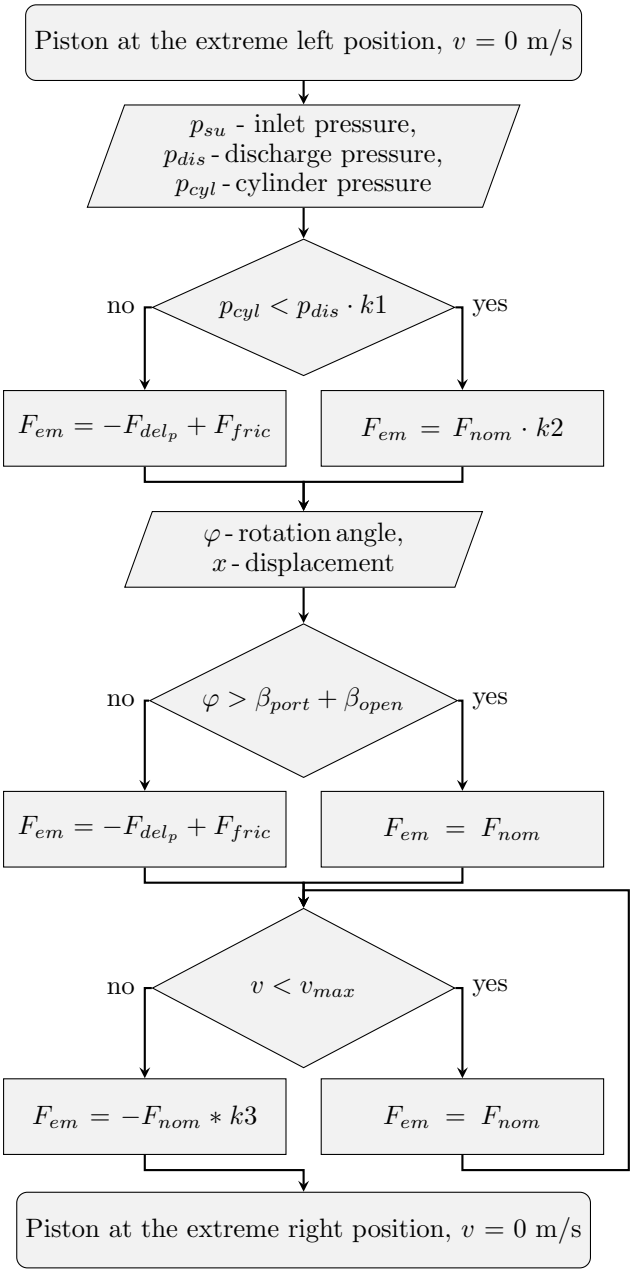

Fig. 8. Piston linear movement algorithm

4.4 Rotation control

Intake: While the piston starts to move away from its extreme left position, the rotation velocity is ω_0. By applying a decelerating torque of $-T_{nom}$ at the moment defined by $k4$, the rotation decreases, ideally down to zero ($k5 = 0$), when the skirt opening is aligned with the inlet opening. The resulting speed can be adjusted by the coefficient $k5$ if the rotation should not be completely stopped but just reduced to allow a higher piston response. This is an open loop control since a high positioning accuracy is not required.

The piston travels to the right without rotation. When the displacement reaches a certain value defined by $k6$, the rotation is accelerated with a torque of T_{nom} in order to close the inlet port when it is dictated by the thermodynamic model.

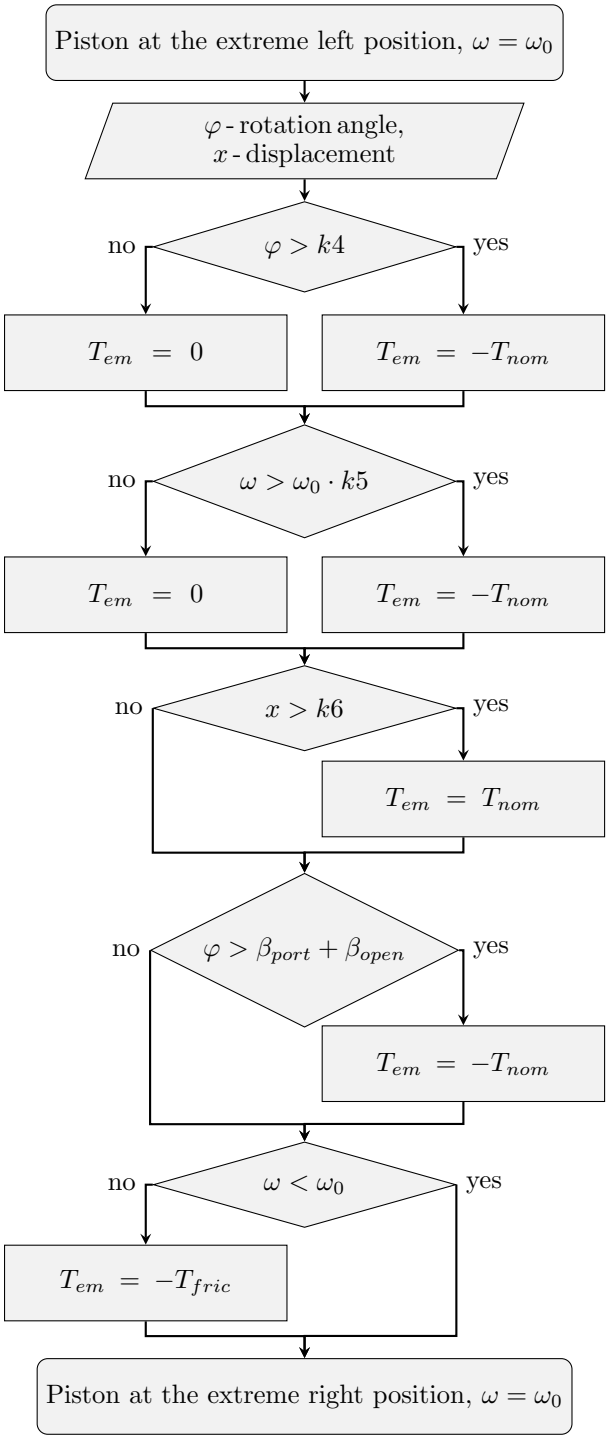

Fig. 9. Piston rotation algorithm

Deceleration After the inlet is closed ($\varphi > \beta_{port} + \beta_{open}$), the piston rotation speed needs to be reduced until it reaches ω_0, then the piston rotates with a constant speed. The torque applied from the servo motor is equal to the one caused by friction. At the end of the stroke, a PI-action can be applied for a better accuracy.

The resulting velocity profile vs. time is shown on Fig.12. It can be seen that the higher the inlet pressure, the faster the piston reaches its maximal translation speed, so a lower brake force is needed to decelerate it until the extreme right position.

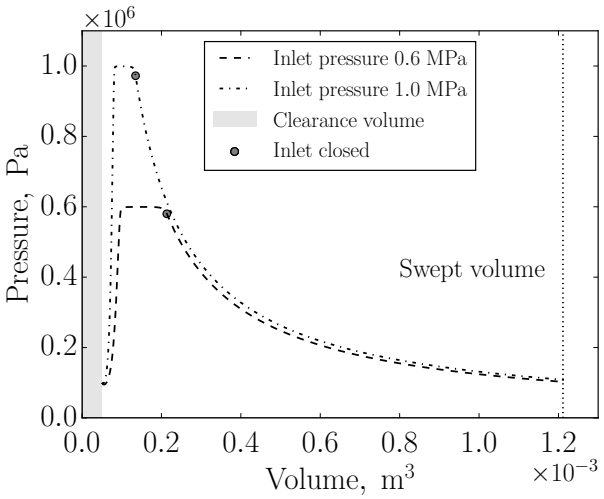

Fig. 10. Piston velocity vs. displacement

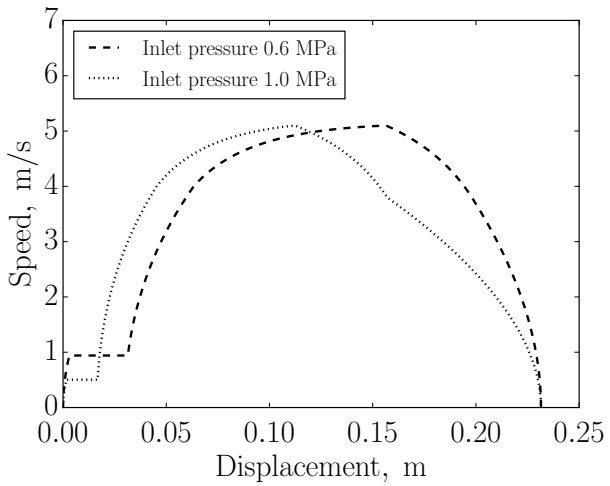

Fig. 11. Piston velocity vs. displacement

Two inlet pressures 1.0 MPa and 0.6 MPa are compared and the configuring factors are identified (Fig. 10).

By performing such simulations within the expected inlet pressure range with a certain step, a matrix of these parameters can be obtained and used in real time to adjust the piston movement under varying inlet pressure.

4.5 Parameters description

Variables: Inlet pressure

Constants: Inlet temperature, outlet pressure, expander geometry, zero piston velocity at the end of expansion phase.

Adjustable parameters: k1, k2, k3, k4, k5, k6.

Efficiency indicators: frequency, filling factor, intake efficiency, power output: to maximize.

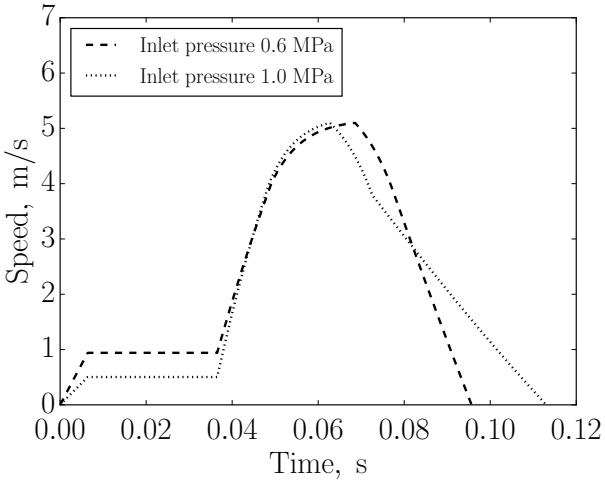

Fig. 12. Piston velocity vs. displacement

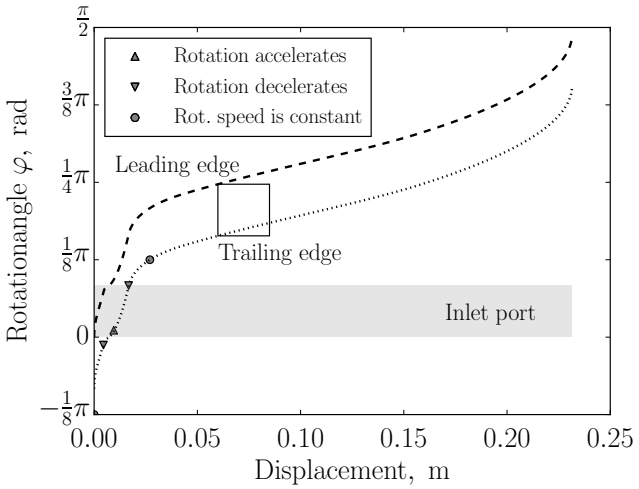

Fig. 13. Piston velocity vs. displacement

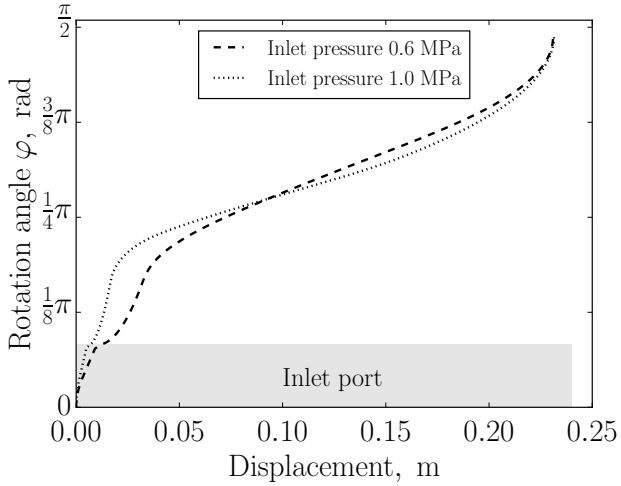

Fig. 14. Piston velocity vs. displacement

5. RESULTS AND DISCUSSIONS

The developed model is based on parameters of the selected linear motor and the servomotor and allows to synchronize the rotation with the linear movement of the expander. By decreasing the linear speed during the intake phase, the pressure loss at the inlet can be reduced. However, reduced translation speed means lower frequency and the mass flow rate through the expander, so the optimum has to be found (Fig. 12).

The rotation of the piston can be increased or decreased when necessary for a better fit of the inlet. A moderate rotating acceleration/deceleration is achievable in combination with the piston deceleration during the intake. The final deceleration must be adjusted so the leading edge of the skirt opening reaches the outlet port at the end of the stroke. In this case this angle is $\pi/2$ (Fig. 13). Two rotation/translation profiles for different inlet pressures are shown on Fig. 14

The shape of the inlet port needs to be adjusted to "follow" an optimal intake profile in order to keep the inlet intersection area around its maximum during the intake phase. Otherwise higher pressure ratios will require high dynamics from electromagnetic train or will cause relatively high intake losses.

The presented model is focused on the inlet control and therefore simplified by setting the outlet pressure as constant.

6. CONCLUSIONS

The dynamics of the system depend on the linear generator used. Industrial linear motors are characterized by large moving masses. It is possible to reduce the weight of the piston if magnets are directly attached to it. A high dynamics of the piston movement is necessary to increase the resulting frequency and the volumetric flow rate of the machine. A relatively high static force is required to keep the piston under control at its extreme positions. The use of a position encoder ensures the high accuracy of the inlet timing, which is crucial for the system efficiency.

The proposed system contains no bouncing devices such as gas- or mechanical springs, which are typically used in free piston machines. Instead, the piston movement is fully controlled, so its velocity becomes zero at both extreme positions. A higher system efficiency is expected since mechanical wear or thermodynamic irreversibilities are avoided.

REFERENCES

Bell, I.H., Wronski, J., Quoilin, S., and Lemort, V. (2014). Pure and pseudo-pure fluid thermophysical property evaluation and the open-source thermophysical property library coolprop. *Industrial & engineering chemistry research*, 53(6), 2498–2508.

Gusev, S., Ziviani, D., De Viaene, J., Derammelaere, S., and van den Broek, M. (2016). Modelling and preliminary design of a variable-bvr rotary valve expander with an integrated linear generator. In *Proceedings of the 17th International Refrigeration and Air Conditioning Conference at Purdue*.

Imran, M., Usman, M., Park, B.S., and Lee, D.H. (2016). Volumetric expanders for low-grade and waste heat recovery applications. *Renewable and Sustainable Energy Reviews*, 57, 1090–1109.

Lemort, V., Quoilin, S., Cuevas, C., and Lebrun, J. (2009). Testing and modeling a scroll expander integrated into an organic rankine cycle. *Applied Thermal Engineering.*, 29, 3094–3102.

Mikalsen, R. and Roskilly, A. (2008). The design and simulation of a two-stroke free-piston compression ignition engine for electrical power generation. *Applied Thermal Engineering*, 28(56), 589–600.

Petrichenko, D., Tatarnikov, A., and Papkin, I. (2015). Approach to electromagnetic control of the extreme positions of a piston in a free piston generator. *Modern Applied Science*, 9(1), 119–128.

Tran, X.B. and Yanada, H. (2013). Dynamic friction behaviors of pneumatic cylinders. *Intelligent Control and Automation*, 4(2).

Appendix A. NOMENCLATURE

A.1 Latin characters

D	diameter	(m)
F	force	(N)
L	length	(m)
m	mass	(kg)
n	number of ports	(-)
p	pressure	(Pa)
S	intersection area	(m^2)
t	time	(s)
V	volume	(m^3)
x	displacement	(m)

A.2 Greek characters

β	port angle	(rad)
Δ	difference	(-)
υ	speed	(m/s)
φ	angle of rotation	(rad)
ϕ	filling factor	(-)
χ	relative displacement	(-)

A.3 Subscript

cyl	cylinder
dis	discharge
el	electromagnetic
fr	friction
max	maximal
min	minimal
open	opening
port	port
rot	rotation
su	supply